RAPID COMMUNICATIONS

The purpose of this Rapid Communications section is to provide accelerated publication of important new results in the fields regularly covered by Journal of Materials Research. Rapid Communications cannot exceed four printed pages in length, including space allowed for title, figures, tables, references, and an abstract limited to about 100 words.

Face-centered-cubic to hexagonal-close-packed transformation in nanocrystalline Ni(Si) by mechanical alloying

M.K. Datta, S.K. Pabi, and B.S. Murty[a)]
Department of Metallurgical and Materials Engineering, Indian Institute of Technology, Kharagpur-721 302, India

(Received 7 August 1999; accepted 27 March 2000)

An allotropic transition from face-centered-cubic (fcc) to hexagonal-close-packed (hcp) Ni(Si) solid solution in $Ni_{95}Si_5$ and $Ni_{90}Si_{10}$ during nanocrystallization by mechanical alloying is reported. The transformation was identified as a defect-induced melting accompanied by a volume expansion of 8.6% and was observed when fcc Ni(Si) reached a critical crystallite size of 10 nm. Calculation based on equation of state showed that a 37% reduction in tetragonal shear modulus and a negative pressure of about 8.7 GPa were generated at the onset of transformation.

Crystal to amorphous transformation can be induced in a wide range of materials by various solid-state techniques such as high-energy particle irradiation, ion-beam mixing, annealing of diffusion couples, hydrogen charging, and high-energy ball milling.[1,2] Despite this variety of techniques, there appears a common observation that atoms are displaced from their equilibrium lattice sites, causing lattice strain and softening of shear elastic constants during the progress of amorphization.[2] According to Lindemann's melting criterion and the unified approach of melting and amorphization,[3] amorphization would occur when the root-mean-square static atomic displacement reaches a critical value identical at the melting point of the crystal. On the other hand, Tallon[4] has pointed out that shear elastic constant falls rapidly with an increase in crystal volume and reaches zero at a volume equal to that of the liquid at the melting point. The experimental results[5] have identified that amorphization occurs when the crystal is strained to a material-dependent critical value, and accompanies a large decrease (~40 to 50%) in the shear elastic constant irrespective of the material. The prerequisities of this phase transformation, namely, the static atomic displacement and shear softening, can be obtained by the presence of static disorder in the parent crystal that can be achieved either by accumulation of defects or by forming a supersaturated solid solution by various solid-state techniques.

Mechanical deformation during mechanical alloying (MA) involves the creation and annihilation of a high density of dislocation in the material, resulting in nanocrystalline grains of a special type of grain boundary.[6] As the atomic displacement in the nanocrystalline grain boundary is higher than the interior of the core, it is expected that the grain boundaries have significant effect on shear softening to induce phase transformation in the nanocrystalline state. Therefore, it becomes possible that the nanocrystalline grain surrounded by a disordered layer may transform to amorphous or other crystal structure below a critical crystallite size. Experiments have shown that nanoparticles of a number of elements such as Nb, Mo, Co, W, Ta,[7] and less common metals such as Y, Gd, Tb, Dy, Ho, Er, and Tm[7] have shown structures other than their equilibrium ones. It is well known that face-centered-cubic (fcc) Ni does not show any polymorphism in the bulk state. However, ion irradiation studies[8,9] demonstrated that Ni can have a metastable hexagonal-close-packed (hcp) structure. The phase transitions from loose-packed structures to close-packed structures during nanocrystallization can be understood by thermodynamic consideration.[7] However, the transitions between close-packed structures are less studied.[10] The present study reports the formation of hexagonal phase on nanocrystallization during mechanical alloying of $Ni_{95}Si_5$ and $Ni_{90}Si_{10}$ and a possible mechanism for this phase transformation is suggested.

Pure Ni and elemental blends of Ni and Si powders of nominal composition $Ni_{95}Si_5$ and $Ni_{90}Si_{10}$ were subjected to high-energy ball milling using a planetary ball mill (Fritsch Pulverisette P-5, Fritsch GmbH, Idar-Oberstein, Germany). The milling was carried out in toluene at 300 rpm up to 50 h in a tungsten carbide vial using 10-mm-diameter tungsten carbide balls with a ball-to-powder weight ratio of 10:1. The milling was interrupted at regular intervals of 5 h to analyze the milled

[a)]Present address: National Research Institute for Metals, Tsukuba 305-0047, Japan.

powder by a Philips 1710 (Philips Analytical, Almelo, The Netherlands) x-ray diffractometer using Co K_α radiation. The thermal behavior of the final milled powder was studied by differential scanning calorimetry (DSC) and isothermal treatments were carried out in the range 373–673 K for 4 h in evacuated glass capsules (~10^{-5} torr) followed by characterization using x-ray diffraction (XRD). The DSC experiments were performed in a Perkin-Elmer 2C unit under high-purity Ar atmosphere at a heating rate of 10 K/min. The effective crystallite sizes of mechanically alloyed powders as well as heat-treated products were calculated by the Voigt function using the single-line method after eliminating the strain and the instrumental broadening contribution.[11] The effective crystallite size of different phases and the volume fraction[12] of these phases have been calculated from their most intense peaks in the XRD patterns.

XRD patterns of $Ni_{95}Si_5$ at different milling times are shown in Fig. 1. The diffraction peaks of Si have disappeared after 10 h of milling, suggesting the formation of fcc solid solution of Si in Ni [Ni(Si)]. The increased incorporation of Si into Ni is known to decrease the lattice parameter of the later.[13] However, it is interesting to note that the position of Ni(Si) peaks continuously shifted to lower angles accompanied by gradual broadening with milling time, indicating a continuous increase in the unit cell volume with refinement of crystallite size. After 30 h of milling, new XRD peaks have been detected (Fig. 1), which were successfully indexed as hexagonal Ni(Si) of molar volume 7.57 cm^3/mol with $a = 0.2603$ nm and $c = 0.4287$ nm. The volume fraction of hcp phase was found to increase from 0.6 to 0.7 when the milling was continued from 30 h to 50 h as calculated from the ratios of integrated intensities[12] of the hcp and fcc XRD peaks. Rietveld analysis of the XRD pattern after 40 h of milling (Fig. 2) has confirmed the presence of hcp phase with $a = 0.2622$ nm and $c = 0.4321$ nm. The volume fraction of the hcp phase at this stage was found to be 0.64 from the Rietveld analysis. Similar phase transformation has been identified in $Ni_{90}Si_{10}$, as shown in the 50-h-milled sample of Fig. 1. Figure 3 shows the variation of molar volume of fcc and hcp Ni(Si) with the refinement of crystallite size. A molar volume expansion of 0.38 cm^3/mol (5.8%) is evident for fcc Ni(Si) when the crystallite size decreased from the bulk state to 10 nm. At this stage, hcp Ni(Si) forms with a sudden increase in the molar volume by 0.60 cm^3/mol (8.6%). The molar volume and crystallite size of the hcp phase increased marginally with the increase of milling time (Fig. 3).

In contrast to the above two samples, formation of hcp phase could not be detected in pure Ni even after milling up to 50 h, as shown in Fig. 1. The crystallite size of Ni decreased at a slower rate with milling time when compared to Ni(Si) and reached only 40 and 21 nm after 30 and 50 h of milling, respectively. It is interesting to

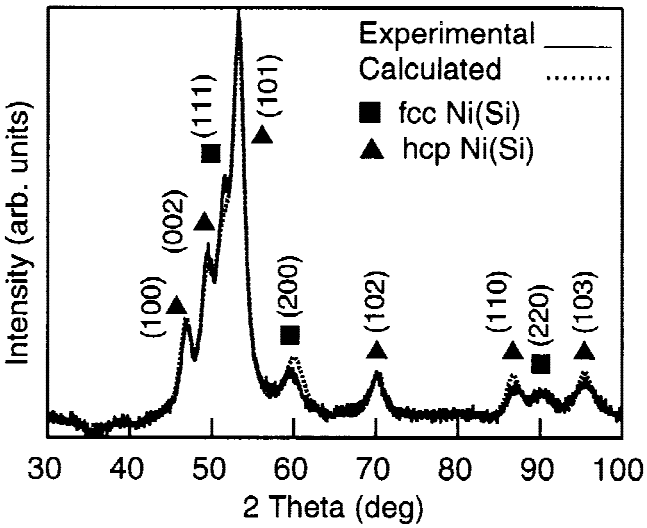

FIG. 2. Rietveld analysis of XRD data of 40-h-milled $Ni_{95}Si_5$.

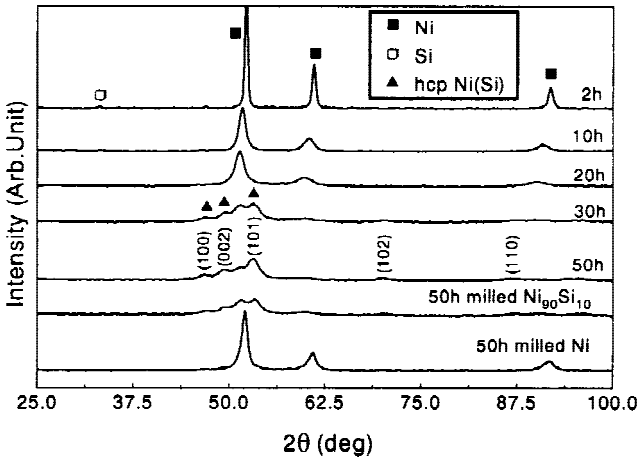

FIG. 1. Comparison of XRD patterns of $Ni_{95}Si_5$ at different milling times with 50-h-milled $Ni_{90}Si_{10}$ and Ni.

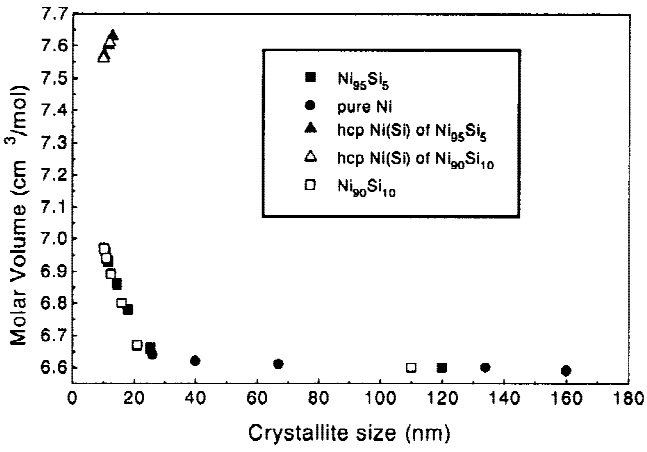

FIG. 3. Variation of molar volume with crystallite size.

note that a small amount of Si dissolved in Ni changes the work-hardening characteristics of Ni such that fragmentation dominates welding during ball milling, which leads to easy nanocrystallization in the case of Ni(Si) in comparison to Ni. Similar results have earlier been obtained in Cu–Ni system.[14] A comprehensive observation of the molar volume variation with the crystallite size of Ni(Si) and Ni (Fig. 3) suggests that the molar volume increases rapidly only when the crystallite size decreases below 10 nm. The crystallite size (21 nm) of pure Ni after 50 h of milling appears to be insufficient to induce fcc to hcp transformation in it, in contrast to $Ni_{95}Si_5$ and $Ni_{90}Si_{10}$. The molar volume change associated with the transformation appears to be characteristic of this transformation and not sensitive to the composition of the blend.

In order to study the phase restoration from metastable hcp to fcc Ni(Si), the sample of $Ni_{95}Si_5$ milled for 50 h has been subjected to DSC. The DSC plot exhibits one sharp exothermic peak at about 663 K (Fig. 4). The enthalpy associated with this exothermic peak is about 5.4 kJ/mol, which is 30% of heat of fusion of Ni (17.48 kJ/mol) and is close to that expected (33%) for such a transition.[5] The XRD patterns of the 50-h-milled sample of $Ni_{95}Si_5$ after heat treatment for 4 h at different temperatures are shown in Fig. 5. At 573 K, hcp phase suddenly transformed to fcc phase with a molar volume and crystallite size of 6.61 cm^3/mol and 46 nm, respectively. The variation of molar volume and crystallite size of hcp and fcc phases with the heat-treatment temperature is shown in Table I. It is interesting to note that the crystallite size of fcc Ni(Si) changes rapidly after the transformation of hcp phase to the former, suggesting the role of interphase interfaces in restricting the grain growth in nanocrystalline materials.

The increase in the molar volume of fcc phase with refinement of crystallite size is expected from the well-known fact that the interatomic spacing of nanocrystal increases continuously from core to surface due to lattice softening.[15,16] Therefore, it is expected that the molar volume at grain boundary will be higher than the calculated weighted average molar volume. Though the molar volume of fcc phase at the time of phase transformation is lower (6.97 cm^3/mol) than that at the melting point of pure Ni (7.05 cm^3/mol), the grain boundary may reach this value due to lattice softening. Hence, the fcc phase at the nanocrystalline grain boundary is expected to undergo a defect-induced melting (Lindemann's melting criterion) to amorphous (liquid) state of zero shear modulus, which relaxes (crystallizes) into a more compatible metastable hcp structure of molar volume 7.57 cm^3/mol, which is in good agreement with the molar volume of liquid at the melting point of Ni (7.55 cm^3/mol). Figure 6 shows the variations of tetragonal shear modulus, $\frac{1}{2}(C_{11} - C_{12})$, with volume strain, calculated based on the equation of state.[17] A 37% reduction in shear modulus (from 49 to 31 GPa) of nanocrystalline Ni has been identified at the onset of transformation, suggesting defect-induced melting.

It is well known that structural changes into dense crystalline structues in bulk state can be brought out under high hydrostatic pressure.[18] Similarly, a negative hydrostatic pressure is expected to result in the reverse process, resulting in a less dense structure.[19] An increase of unit cell volume of fcc phase with refinement of crys-

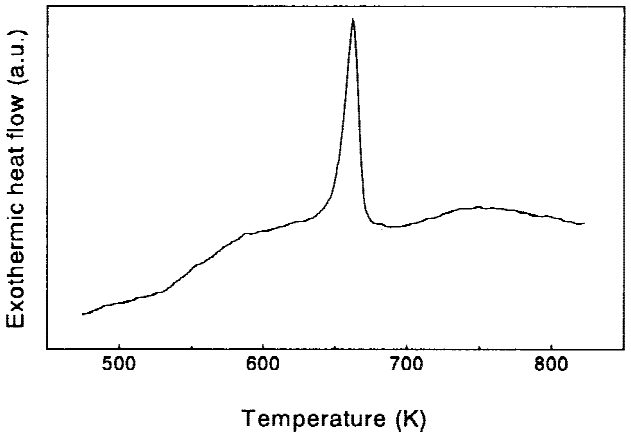

FIG. 4. DSC trace of $Ni_{95}Si_5$ after 50 h of milling.

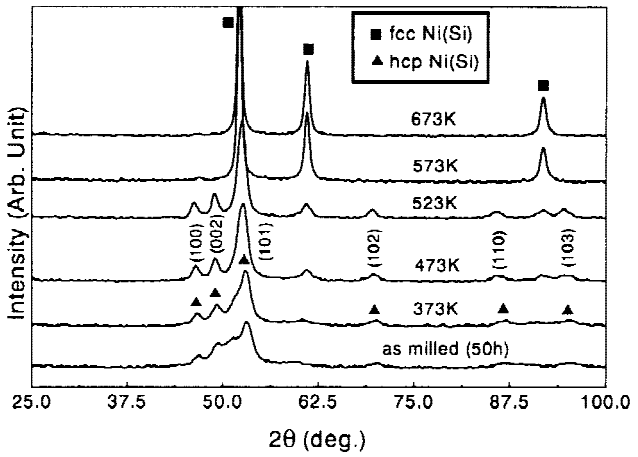

FIG. 5. XRD patterns of samples of $Ni_{95}Si_5$ heat-treated at different temperatures for 4 h.

TABLE I. Molar volume in cm^3/mol (first row for each phase) and crystallite size in nm (second row for each phase) of fcc and hcp Ni(Si) phases after heat treatment at different temperatures for 4 h.

	Temperature (K)				
Phase	423	473	523	573	673
fcc	6.65	6.63	6.62	6.61	6.60
Ni(Si)	15.7	18.4	20.86	46	56
hcp	7.69	7.76	7.82	···	···
Ni(Si)	14.2	17.8	28	···	···

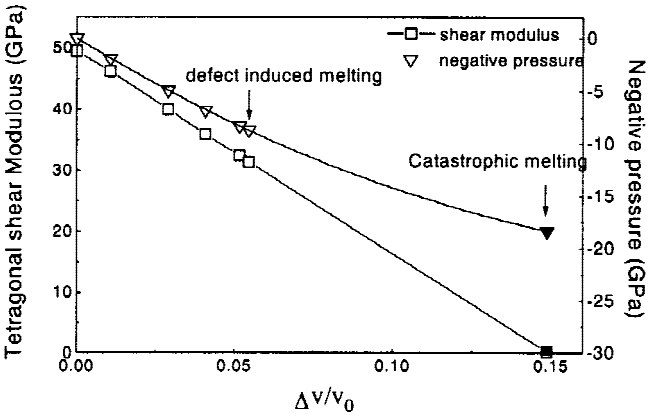

FIG. 6. Variation of shear modulus and negative pressure as a function of excess volume.

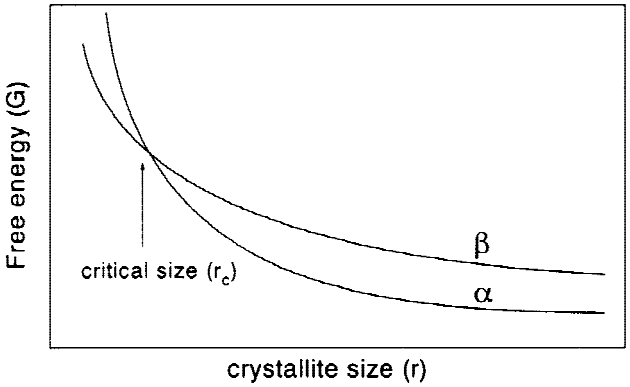

FIG. 7. Schematic free energy diagram showing the relative stability of phase α and phase β with crystallite size.

tallite size develops a negative hydrostatic pressure (isotropic tension). For a stable nanoparticle of radius r, the excessive pressure $P-p$ must be equal to $2\gamma/r$, where P and p are the negative and atmospheric pressures, respectively, and γ is the surface energy. This suggests that with the refinement of crystallite size, the excessive pressure increases. At a critical crystallite size r_c, the excessive pressure reaches the value corresponding to that at the melting point, resulting in the melting of the crystal or transformation to a phase of lower surface energy to reduce the excessive pressure. Calculations based on the equation of state[20] show that a negative hydrostatic pressure of about 8.7 GPa has been generated in fcc Ni(Si) before its transformation to hcp structure, as shown in Fig. 6. Figure 6 also shows that a negative pressure of 18 GPa and a volume strain of about 14% are required for catastrophic melting of Ni. At the time of transformation, total enthalpy change should be equal to $P\Delta V$. Substitution of $P = 8.7$ GPa and $\Delta V = 0.60\ \mathrm{cm}^3/\mathrm{mol}$, yields an enthalpy change of 5.2 kJ/mol, which is in good agreement with the DSC result.

Finally, the thermodynamic condition for phase α to be stable in bulk material over metastable phase β is that $G_\alpha < G_\beta$ (G, Gibb's free energy per unit volume). In case of nanocrystalline materials, the contribution of surface term ($\gamma S/V$) to the free energy cannot be neglected. Here, γ is the surface energy per unit area, and S and V are the surface area and volume, respectively, of the nanoparticle. In a nanocrystalline state, β may become stable if, $G_\alpha + \gamma_\alpha S_\alpha/V_\alpha > G_\beta + \gamma_\beta S_\beta/V_\beta$.[7] In other words, if the rate of increase of free energy with decrease in crystallite size of α phase is higher than that of β phase, β phase will become stable over α phase below a certain crystallite size (r_c) as shown in Fig. 7. The above condition implies that with decreasing crystallite size, the phase with lower surface energy and higher volume becomes energetically favored. If a relatively loosely packed bcc structure is stable in bulk state, a structural transition to tightly packed fcc or hcp structures (lower surface energy) becomes possible on nanocrystallization. On the other hand, structural changes in the nanocrystalline state of close-packed structures (surface energies are comparable) could be possible by an increase of volume. The transformation of fcc Ni(Si) to hcp Ni(Si) with an accompanied increase in volume is supported by the above hypothesis.

ACKNOWLEDGMENT

The authors wish to thank Dr. M. Ohnuma for his help with the Rietveld analysis.

REFERENCES

1. C.C. Koch, O.B. Cavin, C.G. MacKamey, and J.O. Scarbourgh, Appl. Phys. Lett. **43,** 1017 (1983).
2. W.L. Johnson, M. Li, and C.E. Krill III, J. Non-Cryst. Solids **156–158,** 481 (1993).
3. A. Voronel, S. Rabinovich, A. Kisliuk, V. Steinberg, and T. Sverbilova, Phys. Rev. Lett. **60,** 2402 (1988).
4. J.L. Tallon, Nature (London) **342,** 658 (1989).
5. J. Koike, Phys. Rev. B **47,** 7700 (1993).
6. H.J. Fecht, Nanostruct. Mater. **6,** 33 (1995).
7. V.G. Grayznov and L.I. Trusov, Prog. Mater. Sci. **37,** 289 (1993).
8. G. Was, Prog. Surf. Sci. **32,** 211 (1989).
9. Z.J. Zhang, H.Y. Bai, Q.L. Qiu, T. Yang, K. Tao, and B.X. Liu, J. Appl. Phys. **73,** 1702 (1993).
10. V. Blaaderen, R. Ruel, and P. Wiltzius, Nature (London) **385,** 321 (1997).
11. Th. H. de Keijeer, J.I. Langford, E.I. Mittemeijer, and A.B.P. Vogels, J. Appl. Crystallogr. **15,** 308 (1982).
12. B.D. Culity, *Elements of X-ray Diffraction,* 2nd ed. (Addison-Wesley, New York, 1978), p. 411.
13. W.B. Pearson, *A Handbook of Lattice Spacing and Structures of Metals and Alloys* (Pergamon, London, 1958), p. 786.
14. B.S. Murty, D. Das, I. Manna, and S.K. Pabi (unpublished).
15. X.D. Liu, H.Y. Zhang, K. Lu, and Z.Q. Hu, J. Phys. Condens. Matter **6,** L497 (1994).
16. S. Onodera, J. Phys. Soc. Jpn. **61,** 2190 (1992).
17. J.L. Tallon, J. Phys. Chem. Solids. **41,** 837 (1980).
18. P.F. McMillan, Nature (London) **391,** 539 (1998).
19. P. Richet, Nature (London) **331,** 56 (1988).
20. H.J. Fecht, Phys. Rev. Lett. **65,** 610 (1990).